Report on the Third and Final Phase of SNO

R.G. Hamish Robertson

Center for Experimental Nuclear Physics and Astrophysics, University of Washington, Seattle, WA, 98195, USA

E-mail: rghr@u.washington.edu

SNO Collaboration

Abstract. The Sudbury Neutrino Observatory was designed to operate in three distinct configurations that made use of different techniques for measuring the rate of the neutral-current disintegration of deuterium by solar neutrinos. In the third of these phases an array of ^{3}He-filled proportional counters was deployed in the heavy water, and neutrons from the neutrino-induced breakup of deuterium were detected when they captured on ^{3}He, liberating 764 keV of energy in the form of ionization of the gas. Aspects of the analysis of the data from this phase are described, and the results presented. There is good agreement with the results obtained with the other techniques in previous phases, and improved precision on the determination of the "solar" mixing angle.

1. Introduction

Heavy water, D_2O, is an interesting and useful target for the study of the solar neutrino flavor composition and spectrum because there are 3 different reactions induced by neutrinos:

$$\begin{aligned} \nu_e + d &\rightarrow e^- + p + p \quad \text{CC} \\ \nu_x + d &\rightarrow \nu_x + n + p \quad \text{NC} \\ \nu_x + e^- &\rightarrow \nu_x + e^- \quad \text{ES} \end{aligned}$$

Only electron neutrinos produce charged-current interactions (CC), while the neutral-current (NC) and elastic scattering (ES) reactions have sensitivity to non-electron flavors. The NC reaction measures the total flux of all active neutrino flavors above a threshold of 2.2 MeV.

The Sudbury Neutrino Observatory (SNO) detector made use of 10^6 kg of ultrapure 99.92%-enriched D_2O provided on loan by Atomic Energy of Canada Ltd. and Ontario Power Generation. The heavy water was contained in a spherical acrylic vessel 12 m in diameter surrounded by approximately 9500 Hamamatsu R1408 photomultipliers (PMTs) mounted on a geodesic structure 17.8 m in diameter. A mass of about 7×10^6 kg of pure light water shielded and supported the heavy-water target. Details of the detector design can be found in ref. [1].

The SNO detector was configured to operate in 3 distinct phases, the first with pure heavy water [2–4], the second in which 1960 kg of NaCl was dissolved in the heavy water to enhance neutron capture [5, 6], and the third in which an array of proportional counters filled with an 85:15 mixture of ^{3}He and CF_4 was deployed in the heavy water to detect neutrons. A total of 40 'strings' of proportional counters were attached to anchor points on the inner surface of the

vessel on a 1 m square grid. The strings, laser-welded assemblies of individual counters 2 to 3 m in length, had lengths of 9 to 11 m. Four strings contained ^{4}He instead of ^{3}He for assessment of backgrounds. A description of the design and deployment of this 'NCD' (Neutral Current Detection) array, can be found in ref. [7]. The results obtained from SNO's third phase are given in ref. [8] and supplemented here with additional detail.

2. Data

Data were acquired between November 27, 2004 and November 28, 2006 with the NCD array, for a total livetime of 385.17 days. Diverse calibrations were also carried out to aid in tracking the performance and stability of both the PMT and NCD systems, and to aid in analysis. Calibration sources could be deployed on two orthogonal planes bisecting the NCD array. The following sources were used:

(i) Two ^{252}Cf neutron sources, one of which is of precisely determined strength [6].

(ii) An ^{241}AmBe neutron source.

(iii) A ^{16}N source. The 6.13-MeV gammas from this source are the primary calibration of the PMT energy scale [9].

(iv) A ^{8}Li source for calibration of event reconstruction and tests of instrumental cuts.

(v) Encapsulated Th and dissolved ^{222}Rn sources for background calibration.

(vi) Two ^{24}Na sources. Neutron activated NaCl, precisely standardized by gamma counting, was dissolved in the heavy water in October 2005 and October 2006. The 2.754-MeV gammas photodisintegrate deuterium and create a source of neutrons that, like the neutrons produced by neutrino interactions, is nearly uniform and homogeneous. Small corrections were applied for edge effects at the vessel wall, and there is an uncertainty arising from possible lack of mixing homogeneity. These sources are the primary calibration of NCD neutron efficiency.

(vii) A diffusing ball illuminated with laser light was used to calibrate the optical response of the PMT array and to extract the exact positions of the NCDs from their shadows on the PMTs.

In addition, electronic calibrations with pulser signals were carried out regularly on both the PMTs and NCDs.

3. Analysis Procedure

The extraction of the NC signal rate from the NCD array data begins with the selection of good runs, generally runs that are at least 30 minutes in duration, and without abnormalities. A total of 1834 neutrino runs were selected for the blind data and another 121 as an open data set. Six of the ^{3}He strings were rejected from the final data because of mechanical and electrical problems. K5 contained one counter that leaked into the interspace between counters (but not into the heavy water), resulting in gain drift. K2 and M8 had intermittent connections to their cables. J3 and N4 had an excess of low-amplitude events possibly caused by an intermittent connection. K7 exhibited fluctuating gain.

The PMT and NCD data contained instrumental or irrelevant events that were removed by a set of algorithms and cuts. For the PMT data, the cuts are as described in [4] with some minor revisions. Instrumental backgrounds such as bursts, oscillatory events caused by electromagnetic transients, 'fork' events caused by microdischarge in insulators (mainly near the tops of the delay lines), and blank digitizer traces were removed from the NCD data with cuts that permitted an evaluation of the signal loss and residual background. An example of these cuts is shown in Fig. 1.

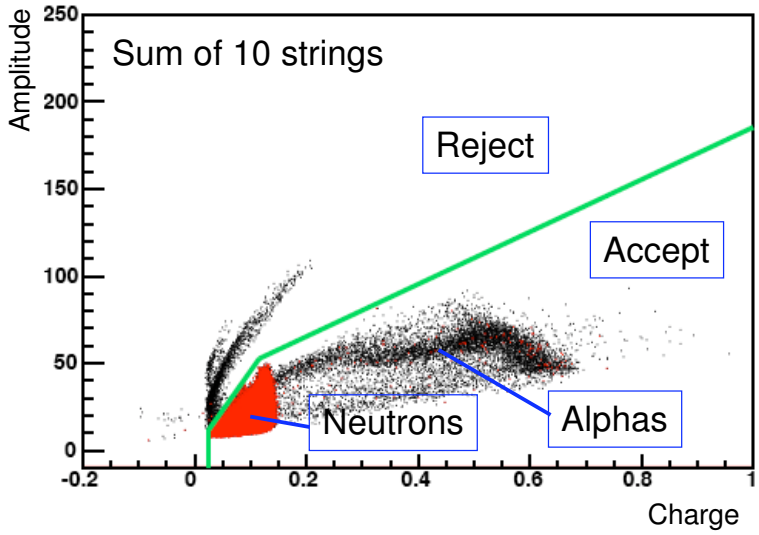

Figure 1. Cuts used to eliminate events with an anomalous amplitude-to-charge ratio. Such events are generally lacking an ionization tail and thus not coming from standard ionization processes in the gas of the NCD counters. They are often caused by the charge and discharge of fibers and dust motes adhering to insulating surfaces.

The remaining events consisted of neutrons and alpha particles, plus possibly a low-energy component of the type seen in J3 and N4. The alpha spectrum shape was simulated numerically in a detailed model of the physics and electronics responsible for the ionization profiles registered in the digitizers. Neutron spectra were also simulated, which confirmed the accuracy of the approach, but spectra taken from ^{24}Na runs were used to fit the neutron contribution to the spectrum from neutrino runs. Fig. 2 shows the results of the simulation.

The optical and energy responses and position and directional reconstruction of the PMT array were updated from previous work to include light shadowing and reflection from the NCD array. With improvements to the calibration data analysis and increased high voltage on the PMT array, the introduction of the NCD array did not significantly increase the position or energy reconstruction uncertainties from previous phases. A normalization for the photon detection efficiency based on ^{16}N calibration data and Monte Carlo simulations was used to set the absolute energy scale with an uncertainty of 1.1%.

A table summarizing the neutron and Cherenkov-light backgrounds can be found in [8]. Low levels of ^{214}Bi and ^{208}Tl present in the heavy and light water, NCD counters, and cables can create free neutrons from deuteron photodisintegration, and low-energy Cherenkov events from $\beta-\gamma$ decays. Techniques to determine these backgrounds in the water are described in previous works [3, 10–12].

The background contributions from the NCD array were determined by combining the analyses of the alpha energy spectrum and the time-correlated alpha events in the decay chains. The results from these studies agreed with radioassays of material samples prior to the construction of the NCD array. Alphas from ^{210}Pb-^{210}Po on the NCD tube surfaces can induce ^{17,18}O(α,n) interactions. In addition, *in-situ* analysis of the Cherenkov light disclosed three detectable "hotspots" of elevated radioactivity on two strings, two on K5 and one on K2. The external alpha activities on these and 18 other counters were measured by means of a clamshell proportional flow counter that could be placed around individual NCD counters after

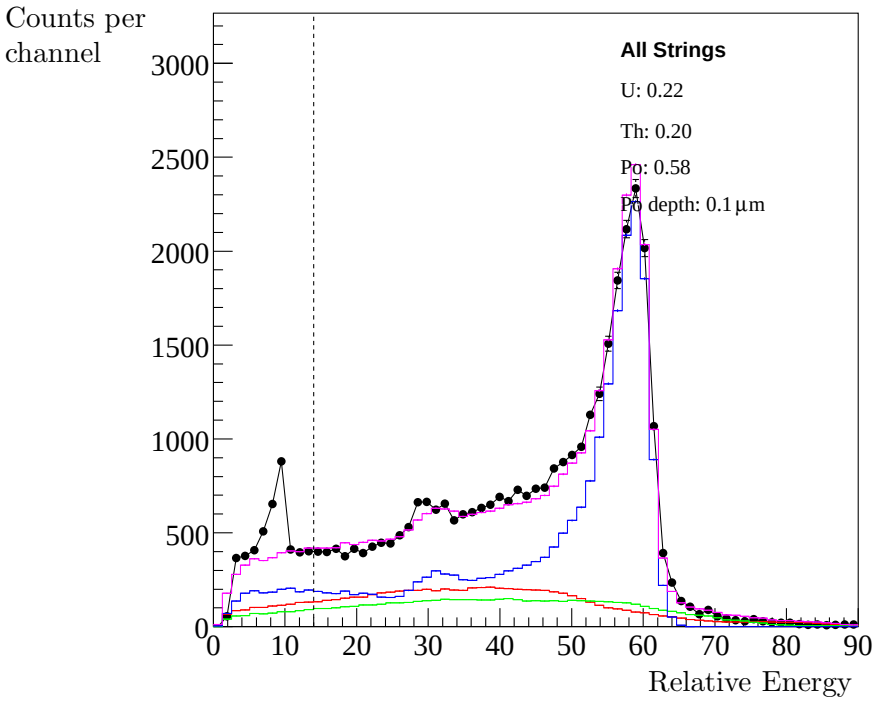

Figure 2. Comparison between a simulation of the NCD alpha spectrum and blind data (a fraction of the neutrino data plus some muon-produced neutrons). The peak near channel 10 is the neutron capture peak at 764 keV, and the peak near channel 60 is dominated by the 5.3-MeV ^{210}Po alpha decay. The simulation is the magenta curve passing through the data points, consisting of the sum of Th-chain (green, lowest curve at channel 30), U-chain (red, next curve) and ^{210}Po alpha activities (blue, next curve), fitted to the data (colors on-line). The U and Th activities have exponential depth profiles in the Ni wall of the NCDs determined from fits to individual string data. The common scale depth for ^{210}Po is 0.1 μm. The fractional contributions of the activities are given in the legend.

they had been removed from SNO, and also by radiochemical assay. Some measurements were also made before deployment. Results from the *in-situ* and *ex-situ* methods gave comprehensive information about the isotopic composition and physical distribution of the activity and yielded the neutron background from the hotspots with an uncertainty less than 0.7% of the NC signal.

Previous results [5,6] reported the presence of neutrons from the acrylic vessel and light water. Measurements with Si counters of alpha radioactivity on the inner surface of the acrylic vessel neck below the normal waterline before and after the NCD phase were consistent with those from the previous phase. Thus, the neutron contribution caused by ^{17,18}O(α,n) and ^{13}C(α,n) at the vessel wall was taken to be the same as for the previous phase. An additional contribution from photodisintegration caused by gammas passing through the vessel wall was determined from the measured ^{214}Bi and ^{208}Tl concentrations in the light water.

Backgrounds from Cherenkov events inside and outside the fiducial volume were estimated using calibration source data, measured activities, Monte Carlo calculations, and controlled injections of Rn into the detector. These backgrounds were found to be small above the analysis threshold of 6.0 MeV effective electron kinetic energy and within the fiducial volume, and were included as an additional uncertainty on the flux measurements. Previous phases identified isotropic acrylic vessel background (IAVB) events, which can be limited to 0.3 remaining IAVB events (68% CL) after data reduction for this phase.

A blind analysis procedure was used to minimize the possibility of introducing biases.

Blindness constraints were removed after all analysis procedures, parameters, and backgrounds were finalized. As described in [8], some minor errors were discovered and corrected after 'box opening.' A simultaneous fit was made for the number of NC events detected by the NCDs, the numbers of NC, CC and ES events detected by the PMTs, and the numbers of background events of various types. A Markov-chain Monte Carlo (MCMC) method was employed to make the fit, which also allowed nuisance parameters (systematics) weighted by external constraints to vary in the fit. The NCD event energy spectrum was fit in the range 0.4 to 1.4 MeV with an alpha background distribution, a neutron calibration spectrum from ^{24}Na data, and two instrumental background event distributions. The PMT events were fit in reconstructed energy, the cosine of the event direction relative to the vector from the sun ($\cos\theta_\odot$), and the reconstructed radial position.

The spectral distributions of the ES and CC events were not constrained to the ^{8}B shape, but were extracted from the data. Fits to the data yielded the following numbers of events: 983^{+77}_{-76} NC (NCD array), 267^{+24}_{-22} NC (PMT array), 1867^{+91}_{-101} CC, and 171^{+24}_{-22} ES, with 185^{+25}_{-22} and 77^{+12}_{-10} neutron background events in the NCD and PMT arrays respectively. Additionally, the total NCD array background fits including alphas and the two instrumental components yielded 6127 ± 101 events.

4. Results

Assuming the ^{8}B neutrino spectrum from [13], the equivalent neutrino fluxes derived from the fitted CC, ES, and NC events are (in units of 10^6 cm^{-2}s^{-1}):

$$\begin{aligned}
\phi^{\rm SNO}_{\rm CC} &= 1.67^{+0.05}_{-0.04}({\rm stat})^{+0.07}_{-0.08}({\rm syst}) \\
\phi^{\rm SNO}_{\rm ES} &= 1.77^{+0.24}_{-0.21}({\rm stat})^{+0.09}_{-0.10}\ ({\rm syst}) \\
\phi^{\rm SNO}_{\rm NC} &= 5.54^{+0.33}_{-0.31}\ ({\rm stat})^{+0.36}_{-0.34}\ ({\rm syst})\ ,
\end{aligned}$$

and the ratio of the ^{8}B neutrino flux measured with the CC and NC reactions is

$$\frac{\phi^{\rm SNO}_{\rm CC}}{\phi^{\rm SNO}_{\rm NC}} = 0.301 \pm 0.033\ ({\rm total}). \qquad (1)$$

Neutrinos from *hep* capture could also be present in the measured fluxes; the SSM contribution would be 0.5%.

The ES flux presented here is 2.2σ lower than that found by Super-Kamiokande-I [14], apparently a downward statistical fluctuation, as evidenced in the shortfall of signals near $\cos\theta_\odot = 1$ in two isolated energy bins. The ^{8}B spectral shape [13] used here differs from that [15] used in previous SNO results. The CC, ES and NC flux results in this Letter are in agreement ($p = 32.8\%$ [16]) with the NC flux result of the D_2O phase [3] and with the fluxes from the salt phase [6].

The fluxes, combined with day and night energy spectra from the pure D_2O and salt phases [6,17], place constraints on neutrino flavor mixing parameters. Two-flavor active neutrino oscillation models are used to predict the CC, NC, and ES rates in SNO. A combined χ^2 fit to SNO D_2O, salt, and NCD-phase data yields the allowed regions in Δm^2 and $\tan^2\theta$ shown in Fig. 3(a). In a global analysis of all solar neutrino data (including Borexino [18] and Super-Kamiokande-I [14]) and the 2881 ton-year KamLAND reactor anti-neutrino results [19], the allowed regions are shown in Fig. 3(b and c). The 3 phases of SNO are here treated as separate experiments with correlations taken into account. A 3-phase unified analysis is in progress. The best-fit point to the solar global plus KamLAND data yields $\Delta m^2 = 7.59^{+0.19}_{-0.21} \times 10^{-5}$ eV^2 and $\theta = 34.4^{+1.3}_{-1.2}$ degrees, where the errors reflect marginalized 1-σ ranges. In our analyses, the ratio f_B of the total ^{8}B flux to the SSM [20] value was a free parameter, while the total *hep* flux was fixed at 7.93×10^3 cm^{-2} s^{-1} [21].

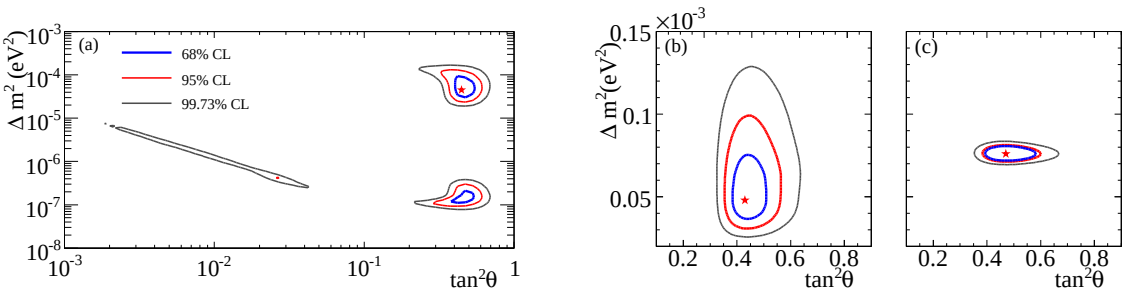

Figure 3. Neutrino-oscillation contours. (a) SNO only: D_2O & salt day and night spectra, NCD phase fluxes. The best-fit point is $\Delta m^2 = 4.57 \times 10^{-5}$ eV^2, $\tan^2\theta = 0.447$, $f_B = 0.900$, with χ^2/d.o.f.=73.77/72. (b) Solar Global: SNO, SK, Cl, Ga, Borexino. The best-fit point is $\Delta m^2 = 4.90 \times 10^{-5}$ eV^2, $\tan^2\theta = 0.437$, $f_B = 0.916$. (c) Solar Global + KamLAND. The best-fit point is $\Delta m^2 = 7.59 \times 10^{-5}$ eV^2, $\tan^2\theta = 0.468$, $f_B = 0.864$.

5. Conclusion

The third and final phase of SNO has made possible a determination of the total flux of active ^{8}B neutrinos from the sun that is independent of the methods of the previous phases. The flux is in agreement with standard solar model calculations and the uncertainty in θ is reduced.

6. Acknowledgments

This research was supported by: Canada: NSERC, Industry Canada, NRC, Northern Ontario Heritage Fund, Vale Inco, AECL, Ontario Power Generation, HPCVL, CFI, CRC, Westgrid; US: Dept. of Energy, NERSC PDSF; UK: STFC (formerly PPARC); Portugal: FCT. We thank the SNO technical staff for their strong contributions.

References

[1] Boger J *et al.* (SNO) 2000 *Nucl. Instrum. Meth.* **A449** 172–207 (*Preprint* nucl-ex/9910016)
[2] Ahmad Q R *et al.* (SNO) 2001 *Phys. Rev. Lett.* **87** 071301 (*Preprint* nucl-ex/0106015)
[3] Ahmad Q R *et al.* (SNO) 2002 *Phys. Rev. Lett.* **89** 011301 (*Preprint* nucl-ex/0204008)
[4] Aharmim B *et al.* (SNO) 2007 *Phys. Rev.* **C75** 045502 (*Preprint* nucl-ex/0610020)
[5] Ahmed S N *et al.* (SNO) 2004 *Phys. Rev. Lett.* **92** 181301 (*Preprint* nucl-ex/0309004)
[6] Aharmim B *et al.* (SNO) 2005 *Phys. Rev.* **C72** 055502 (*Preprint* nucl-ex/0502021)
[7] Amsbaugh J F *et al.* 2007 *Nucl. Instrum. Meth.* **A579** 1054–1080 (*Preprint* 0705.3665)
[8] Aharmim B *et al.* (SNO) 2008 *Phys. Rev. Lett.* **101** 111301–111305 (*Preprint* 0806.0989)
[9] Dragowsky M R *et al.* 2002 *Nucl. Instrum. Meth.* **A481** 284–296 (*Preprint* nucl-ex/0109011)
[10] Andersen T C *et al.* (SNO) 2003 *Nucl. Instrum. Meth.* **A501** 399–417 (*Preprint* nucl-ex/0208010)
[11] Andersen T C *et al.* (SNO) 2003 *Nucl. Instrum. Meth.* **A501** 386–398 (*Preprint* nucl-ex/0208015)
[12] Blevis I *et al.* 2004 *Nucl. Instrum. Meth.* **A517** 139–153 (*Preprint* nucl-ex/0305022)
[13] Winter W T, Freedman S J, Rehm K E and Schiffer J P 2006 *Phys. Rev.* **C73** 025503 (*Preprint* nucl-ex/0406019)
[14] Hosaka J *et al.* (Super-Kamkiokande) 2006 *Phys. Rev.* **D73** 112001 (*Preprint* hep-ex/0508053)
[15] Ortiz C E, Garcia A, Waltz R A, Bhattacharya M and Komives A K 2000 *Phys. Rev. Lett.* **85** 2909–2912 (*Preprint* nucl-ex/0003006)
[16] Valassi A 2003 *Nucl. Instrum. Meth.* **A500** 391–405
[17] Ahmad Q R *et al.* (SNO) 2002 *Phys. Rev. Lett.* **89** 011302 (*Preprint* nucl-ex/0204009)
[18] Arpesella C *et al.* (Borexino) 2008 *Phys. Rev. Lett.* **101** 091302
[19] Abe S *et al.* (KamLAND) 2008 *Phys. Rev. Lett.* **100** 221803 (*Preprint* 0801.4589)
[20] Bahcall J N, Serenelli A M and Basu S 2005 *Astrophys. J.* **621** L85–L88 (*Preprint* astro-ph/0412440)
[21] Bahcall J N, Serenelli A M and Basu S 2006 *Astrophys. J. Suppl.* **165** 400–431 (*Preprint* astro-ph/0511337)